The Astrophysical Journal, 698:L152–L157, 2009 June 20 doi:10.1088/0004-637X/698/2/L152

RHESSI OBSERVATIONS OF THE PROPORTIONAL ACCELERATION OF RELATIVISTIC >0.3 MeV ELECTRONS AND >30 MeV PROTONS IN SOLAR FLARES

A. Y. Shih[1], R. P. Lin[1], and D. M. Smith[2]
[1] Physics Department and Space Sciences Laboratory, University of California, Berkeley, CA 94750, USA; ayshih@ssl.berkeley.edu
[2] Santa Cruz Institute of Particle Physics and Department of Physics, University of California, Santa Cruz, CA 95064, USA
Received 2009 February 25; accepted 2009 May 18; published 2009 June 4

ABSTRACT

We analyze all *RHESSI* measurements from 2002 to 2005 (29 flare events) of the 2.223 MeV neutron-capture γ-ray line and >0.3 MeV electron bremsstrahlung continuum emissions, produced by >30 MeV accelerated protons (depending on assumptions) and >0.3 MeV accelerated electrons, respectively. We find a close proportionality between the two emissions over >3 orders of magnitude in fluence, from the largest flares down to the limits of detectability. This implies that the processes in flares that accelerate electrons above 0.3 MeV and protons above 30 MeV are closely related, and that the relative acceleration of these two populations is roughly independent of flare size. We find an overall weak correlation between the 2.223 MeV fluence and the peak *GOES* 1–8 Å soft X-ray (SXR) flux, but with a close proportionality for flares with 2.223 MeV fluence above a threshold of 50 ph cm^{-2} (equivalent to $\sim 2 \times 10^{31}$ protons >30 MeV). Below this threshold the flares usually have large (M-class or higher) but generally uncorrelated excess SXR emission. Thus, above this threshold it appears that flares reach a maximum efficiency for >30 MeV proton and relativistic (>0.3 MeV) electron acceleration, with proportionate amounts of energy going to flare SXR thermal emission and to >50 keV electrons. Finally, we find that the electron-to-proton ratios—$J_e(0.5\ \mathrm{MeV})/J_p$ (10 MeV)—in these flares, obtained from the γ-ray observations, are about 2 orders of magnitude larger than the ratios in gradual solar energetic particle (SEP) events, but are comparable with ratios in impulsive SEP events.

Key words: acceleration of particles – gamma rays: observations – Sun: flares – Sun: X-rays, gamma rays

1. INTRODUCTION

The Sun accelerates particles during transient releases of energy such as flares and coronal mass ejections (CMEs). Observations of γ-ray lines and pion-decay continuum produced by accelerated ions making nuclear collisions with the ambient solar atmosphere and of hard X-ray (HXR)/γ-ray bremsstrahlung continuum emission produced by accelerated electrons show that ions are accelerated up to ~GeV energies and electrons up to hundreds of MeV, respectively, in large solar flares. Following such flares, ions and electrons up to comparable energies are often detected in situ near 1 AU in intense, gradual solar energetic particle (SEP) events (see Cane et al. 1986), but the delayed onsets and the mostly coronal/solar wind composition and charge states of the SEPs indicate that they are accelerated by shocks driven by associated fast CMEs at altitudes of ~2–40 solar radii (Kahler 1994; Tylka & Lee 2006), and not by flares. In large flares, accelerated $\gtrsim$20 keV electrons and $\gtrsim$ few MeV ions often contain $\gtrsim$10%–50% of the total energy released (Lin & Hudson 1976; Lin et al. 2003; Emslie et al. 2004b, 2005), indicating that particle acceleration and flare energy release mechanisms are intimately related.

From *Solar Maximum Mission* (*SMM*) observations, Vestrand (1988) and Murphy et al. (1993) found a correlation of >0.3 MeV electron bremsstrahlung continuum emission with 4–8 MeV nuclear excess emission and also with the 2.223 MeV neutron-capture line; and Cliver et al. (1994) found a correlation of 4–8 MeV nuclear excess emission with >50 keV continuum emission. Here, we analyze the *RHESSI* measurements (Lin et al. 2002) of γ-ray flares and find a remarkably close linear correlation between the 2.223 MeV γ-ray line fluence and >0.3 MeV electron bremsstrahlung continuum fluence, extending over >3 orders of magnitude in fluence. In general, we find a poor correlation of 2.223 MeV line fluences to SXR peak fluxes, but for flares with 2.223 MeV line fluences above 50 ph cm^{-2}, we again find a close linear correlation.

2. OBSERVATIONS

RHESSI provides imaging and spectroscopy of solar-flare X-ray/γ-ray emissions from ~3 keV to ~17 MeV, utilizing nine rotating modulation collimators (the spacecraft spins at 15 rpm), each in front of a segmented, coaxial germanium detector (GeD). The GeDs are cooled to 80–95 K for a high spectral resolution capable of resolving all γ-ray lines except for the 2.223 MeV line (Figure 1). The GeD front segments absorb nearly all HXR emission below ~0.2 MeV, allowing the rear segments used in this analysis to observe >0.3 MeV γ rays with much lower deadtime. Each photon is individually tagged with its energy and time to a microsecond. Time-coincident events in adjacent detectors ($\lesssim$10% of the total), likely multiple Compton scatters of a single photon, are summed together.

Ideally, a comparison of electron to ion acceleration would have detailed spectral information for both populations. Energetic ions colliding with the solar atmosphere produce excited nuclei, positrons, energetic neutrons, and pions, resulting in the emission of a variety of prompt nuclear de-excitation lines, the positron-annihilation line at 511 keV, the neutron-capture line at 2.223 MeV, and the π° decay feature at ~70 MeV, respectively (e.g., Murphy et al. 2007, 2005, 1987). By measuring the fluxes of several lines with different energy thresholds we can obtain spectral information (e.g., Ramaty et al. 1996), but *RHESSI*'s sensitivity only allows this in the largest flares (e.g., Smith et al. 2003).

We instead focus on the neutron-capture line, usually the most intense line in flares. Energetic neutrons, produced by $\gtrsim$20 MeV nucleon^{-1} ions, thermalize by elastic collisions in

the high-density photosphere (on a timescale of ∼100 s) and then captured by hydrogen to form deuterium while emitting an extremely narrow ($\lesssim$0.1 keV FWHM) line at 2.223 MeV (e.g., Hua & Lingenfelter 1987). The actual ion energy range that produces this line depends on the ion spectral index and accelerated and ambient abundances, and we choose to refer to this population as >30 MeV protons throughout this Letter due to the normalization used in past simulations. *RHESSI*, with ∼4–9 keV FWHM resolution at this energy, can detect it from much weaker flares than any other line and exclude contamination from nearby lines. Since the line is produced deep in the photosphere, we correct for attenuation at large heliocentric angles (using the *RHESSI* HXR source location) due to Compton-scattering by the overlying atmosphere; e.g., at the 73° heliocentric angle of the 2002 July 23 flare, Monte Carlo modeling (Hua & Lingenfelter 1987) estimates ∼53% attenuation of the line flux. The attenuation varies by ∼10%–20% for spectral indices from 2.75 to 4.75, so an index of 3.75 was assumed throughout this study. The corrected flare-integrated line fluence is approximately proportional to the total number of >30 MeV protons. We compare this fluence to the total >0.3 MeV bremsstrahlung fluence, which is proportional to the total number of >0.3 MeV electrons.

We selected flares with significant ($\gtrsim 10\sigma$) emission in the 100–300 keV channel of the *RHESSI* quicklook summary data (Schwartz et al. 2002) or of *GOES* class X1 or higher, occurring before 2006 (when radiation damage of the GeDs became severe). The γ-ray background spectrum during the flare—continuum emission primarily produced in the Earth's atmosphere by cosmic rays or subsequent to passages through the South Atlantic Anomaly—was approximated by averaging the spectra acquired 15 orbits (about 1 day) before and after the flare, when the spacecraft is approximately in the same geomagnetic location (other time periods were chosen when these data were missing or contaminated). Each flare's background-subtracted spectrum was fit over 0.25–8.5 MeV with a photon model including (1) a broken power law for electron bremsstrahlung emission (when significant, the break is typically upward around ∼0.6–0.9 MeV), (2) the positron-annihilation line, the neutron-capture line, and the narrow de-excitation lines represented by Gaussian profiles, and (3) a combination of broad Gaussian profiles to approximate both the broad de-excitation lines and the so-called unresolved nuclear continuum (e.g., Murphy et al. 1990). For weaker flares, statistically insignificant components were then removed. Present uncertainties in the *RHESSI* detector response model may result in a systematic inaccuracy of the bremsstrahlung fluence of $\lesssim$10%.

Table 1 lists all 29 flares with significant ($>3\sigma$) > 0.3 MeV bremsstrahlung fluence, including flares that were not observed completely. Since 2.223 MeV line emission is delayed, flares missing coverage at the beginning (end) will preferentially miss >0.3 MeV bremsstrahlung (2.223 MeV line) emission. We estimate the incomplete-coverage bias on flare ratios of neutron-capture line fluence to >0.3 MeV bremsstrahlung fluence to be $\lesssim$10%, except for the 2003 October 28 flare where the impulsive peak was missed—the *INTEGRAL* observation (Kiener et al. 2006) indicates that the *RHESSI* ratio is ∼40% too large. Three of the *GOES* flares have two distinct intervals of high-energy emission separated by at least 3 minutes, which are listed separately. From Table 1, we excluded from further analysis those flares at heliocentric angles greater than 80° (correction for limb-darkening is too uncertain) and flares with a strong background that cannot be easily subtracted (e.g., produced by SEPs from an earlier flare). Note that down to *RHESSI*'s sensitivity limit, solar flares appear to produce 2.223 MeV line emission if and only if they produce >0.3 MeV bremsstrahlung emission; those flares with negligible 2.223 MeV line fluence in Table 1 are invariably those at large heliocentric angles.

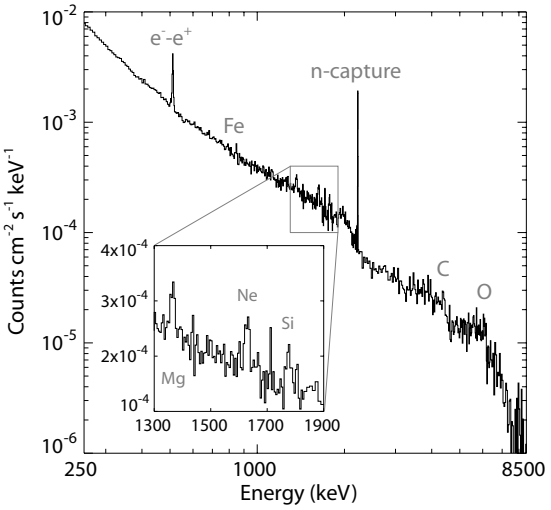

Figure 1. *RHESSI* γ-ray count spectrum of the 2002 July 23 solar flare. The positron-annihilation line (511 keV), the neutron-capture line (2.223 MeV), and six nuclear de-excitation lines are labeled. The narrow line at 1.712 MeV is the single-escape peak of the neutron-capture line.

Figure 2 plots the corrected neutron-capture line fluence, $F_{2.2}$, versus the >0.3 MeV bremsstrahlung fluence, $F_{>0.3\ \mathrm{MeV}}$, for the 18 flares with complete coverage (solid circles) and six with incomplete coverage (solid triangles). Gradual flares (defined as SXR burst duration—peak to 10% of peak flux—greater than 1 hr (see Cane et al. 1986)) have black symbols, while impulsive flares (SXR duration less than 1 hr) are in two colors: red if less than 45 minutes and blue otherwise. The complete-coverage flares fit well (Pearson's correlation coefficient of $r^2 = 0.97$ in log–log space ($r^2 = 0.92$ for all flares)) to a straight line passing through the origin, $F_{2.2} = 0.066\ F_{>0.3\ \mathrm{MeV}}$, over a range of >3 orders of magnitude in fluence. All flares fall ($<1\sigma$) within a factor of 2 of the best-fit line, except for four flares with marginal (~ 1–2σ) line detections. The closeness of this correlation is obtained even though the variability of the proton spectrum and possible directivity of electron bremsstrahlung (e.g., Vestrand et al. 1987) are ignored.

Adding the 1980–1989 γ-ray line flares (Figure 2, open symbols) detected by the *Gamma-Ray Spectrometer* (*GRS*) on *SMM* (Vestrand et al. 1999) still gives a good fit ($r^2 = 0.84$ for all flares, $r^2 = 0.89$ for complete-coverage flares), but several *SMM* flares have 2.223 MeV line fluences above the fit line. Ramaty et al. (1993) pointed out that *GRS* fluences may be contaminated by a broader ^{32}S line at 2.230 MeV because *GRS* has poor energy resolution (∼90 keV), although *RHESSI* has not detected such a line. Some of the greater spread of *SMM* flares may be due to incomplete coverage or due to the time intervals used by Vestrand et al. (1999), but a reanalysis of selected *SMM* flares confirms that the bias is typically $\lesssim 1\sigma$ (G. H. Share 2007, private communication). Recent improvements of the *SMM*/*GRS* response model may also result in changes in the measurements.

Using an isotropic thick-target model, we estimate $N_p(>30\ \mathrm{MeV})$, the number of protons above 30 MeV, assuming

Table 1
List of *RHESSI* Gamma-Ray Flares

Date and Time (UT)	*GOES* Class	Location (°)	Θ (°)	Fluence (ph cm^{-2})			N_p (>30 MeV)	N_e (0.5 MeV)	J_e (0.5 MeV)/
				>0.3 MeV Continuum	2.2 MeV Line	2.2 MeV Line (corrected)	(prot)	(elec MeV^{-1})	J_p(10 MeV)
(1)	(2)	(3)	(4)	(5)	(6)	(7)	(8)	(9)	(10)
2002 Feb 26 10:28	C9.6	S15W80	79.0	28.8 ± 5.6	1.45 ± 0.70	4.3 ± 2.1	2.1 × 10^{30}	1.5 × 10^{33}	7.6 × 10^{2}
2002 May 31 00:16[a]	M2.4	S31E90	>80	63.0 ± 5.8	0.14 ± 0.37	...	...	2.2 × 10^{33}	...
2002 Jul 20 21:30[a]	X3.3	S12E89	>80	429 ± 11	2.2 ± 1.2	...	...	4.0 × 10^{33}	...
2002 Jul 23 00:36	X4.8	S13E71	73.1	4080. ± 13	188.5 ± 3.7	408 ± 18	2.0 × 10^{32}	2.6 × 10^{35}	1.4 × 10^{3}
2002 Aug 20 08:27	M3.4	S11W37	41.2	116 ± 18	1.36 ± 0.90	1.6 ± 1.1	7.8 × 10^{29}	3.4 × 10^{34}	4.5 × 10^{4}
2003 Apr 26 08:07	M7.0	N19W69	72.5	118.6 ± 7.3	1.17 ± 0.98	2.5 ± 1.9	1.2 × 10^{30}	8.1 × 10^{33}	7.3 × 10^{3}
2003 May 27 23:08	X1.4	S07W16	16.7	16.46 ± 0.92	1.93 ± 0.22	1.98 ± 0.23	9.5 × 10^{29}	6.1 × 10^{32}	6.8 × 10^{2}
2003 Jun 17 22:56	M6.8	S08E58	59.2	879 ± 12	45.6 ± 2.3	69.0 ± 3.7	3.3 × 10^{31}	4.1 × 10^{34}	1.3 × 10^{3}
2003 Oct 28 11:10[c,d]	X17	S18E07	23.6	> 16301 ± 21	> 1870. ± 12	> 1977 ± 15	> 9.5 × 10^{32}	> 1.0 × 10^{36}	> 1.1 × 10^{3}
2003 Oct 29 20:50[b]	X10	S19W04	24.2	...	> 292.7 ± 5.7	> 310.3 ± 6.2	> 1.5 × 10^{32}	...	...
2003 Nov 2 17:25[d]	X8.3	S17W56	59.1	> 17.7 ± 1.2	> 465.1 ± 5.0	> 702 ± 13	> 3.4 × 10^{32}	> 5.8 × 10^{35}	< 1.8 × 10^{3}
2003 Nov 3 09:55[s]	X3.9	N08W73	73.1	480. ± 11	3.3 ± 1.4	7.1 ± 3.0	3.4 × 10^{30}	3.1 × 10^{34}	9.6 × 10^{3}
" d,s	"	"	"	> 467 ± 10.	> 11.3 ± 2.0	> 24.9 ± 4.6	> 1.2 × 10^{31}	> 4.0 × 10^{34}	< 3.5 × 10^{3}
2004 Jan 6 06:30[a]	M5.8	N05E89	>80	120.2 ± 4.7	0 ± 0.59	...	...	5.9 × 10^{33}	...
2004 Jul 15 01:41	X1.8	S10E54	55.8	5.70 ± 0.61	0.09 ± 0.15	0.12 ± 0.12	5.9 × 10^{28}	3.3 × 10^{31}	6.0 × 10^{2}
2004 Jul 15 18:24	X1.6	S11E44	46.3	21.8 ± 1.2	0.63 ± 0.27	0.79 ± 0.34	3.8 × 10^{29}	3.7 × 10^{32}	1.0 × 10^{3}
2004 Jul 16 02:07	X1.3	S11E40	42.6	5.3 ± 1.2	0.13 ± 0.16	0.16 ± 0.16	7.7 × 10^{28}	5.6 × 10^{32}	7.7 × 10^{3}
2004 Nov 10 02:13	X2.5	N07W46	46.5	625 ± 12	27.9 ± 2.3	35.2 ± 2.8	1.7 × 10^{31}	4.2 × 10^{34}	2.6 × 10^{3}
2005 Jan 15 23:04[d]	X2.6	N15W07	20.8	> 3046 ± 30.	> 147.6 ± 5.3	> 153.9 ± 5.5	> 7.4 × 10^{31}	> 2.0 × 10^{35}	< 2.9 × 10^{3}
2005 Jan 17 09:52	X3.8	N14W28	33.8	3031 ± 22	115.5 ± 4.9	130.0 ± 5.5	6.2 × 10^{31}	1.3 × 10^{35}	2.2 × 10^{3}
2005 Jan 19 08:23[s]	X1.5	N15W47	50.9	722 ± 13	29.8 ± 2.6	39.4 ± 3.5	1.9 × 10^{31}	3.7 × 10^{34}	2.1 × 10^{3}
" s	"	"	"	2155 ± 18	200.4 ± 4.8	265.3 ± 7.1	1.3 × 10^{32}	7.6 × 10^{34}	6.3 × 10^{2}
2005 Jan 20 07:01	X7.1	N13W58	60.6	16391 ± 25	784.1 ± 8.8	1217 ± 23	5.8 × 10^{32}	6.7 × 10^{35}	1.2 × 10^{3}
2005 Aug 25 04:41	M6.4	N09E78	77.8	860. ± 10.	3.8 ± 1.8	10.6 ± 4.9	5.1 × 10^{30}	3.2 × 10^{34}	6.6 × 10^{3}
2005 Sep 7 17:40[a,b,c,d]	X17	S13E88	>80	...	> 2.43 ± 0.36	...	...	...	...
2005 Sep 9 20:02[c]	X6.2	S15E64	67.9	> 200.9 ± 2.6	> 9.82 ± 0.64	> 17.7 ± 1.2	> 8.5 × 10^{30}	> 1.7 × 10^{33}	> 2.1 × 10^{2}
2005 Sep 10 22:07[s]	X2.1	S10E45	48.1	41.5 ± 1.2	0.28 ± 0.25	0.35 ± 0.32	1.7 × 10^{29}	8.8 × 10^{32}	5.5 × 10^{3}
" d,s	"	"	"	> 108.7 ± 1.9	> 8.80 ± 0.53	> 11.27 ± 0.69	> 5.4 × 10^{30}	> 8.5 × 10^{31}	< 1.7 × 10^{1}
2005 Sep 13 23:23	X1.7	S11E01	18.1	9.66 ± 0.91	0.70 ± 0.21	0.72 ± 0.22	3.4 × 10^{29}	7.6 × 10^{31}	2.3 × 10^{2}

Notes. Column (1): date/time of *GOES* peak flux. Column (2): *GOES* X-ray class. Column (3): location in heliographic coordinates of the *RHESSI* HXR source (°). Column (4): the corresponding heliocentric angle (°). Column (5): $F_{>0.3\ \mathrm{MeV}}$, 0.3–8.5 MeV bremsstrahlung continuum fluence (ph cm^{-2}). Column (6): 2.223 MeV neutron-capture line fluence (ph cm^{-2}). Column (7): $F_{2.2}$, corrected neutron-capture line fluence (ph cm^{-2}). Column (8): calculated number of protons >30 MeV. Column (9): calculated differential number of electrons at 0.5 MeV (electrons MeV^{-1}). Column (10): calculated ratio (dimensionless) of electron flux at 0.5 MeV (electrons cm^{-2} s^{-1} MeV^{-1}) to proton flux at 10 MeV (protons cm^{-2} s^{-1} MeV^{-1}), with inequality signs due to incomplete coverage. Superscript notes: (a) occurred near or over the solar limb, (b) poor background subtraction, (c) missing beginning data, (d) missing end data, and (s) well-separated time interval of high-energy emission within a single *GOES* flare. Flares marked with (a) or (b) are not plotted, and flares marked with (s) are plotted as separate points in Figure 2 and as summed points in Figure 3.

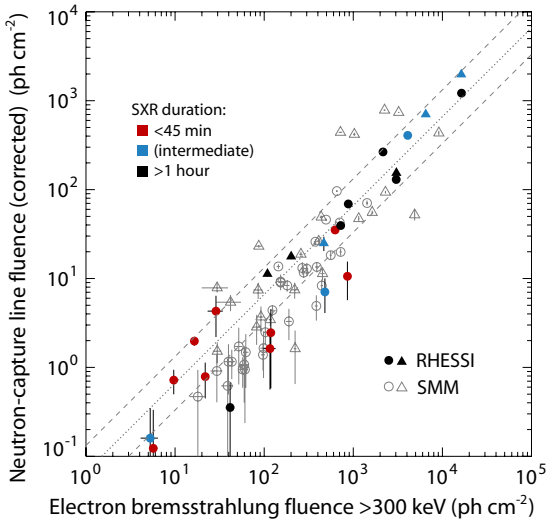

Figure 2. $F_{2.2}$ vs. $F_{>0.3\ \mathrm{MeV}}$ for flares with heliocentric angles $<80°$ (*RHESSI* in solid symbols, *SMM* in open symbols). Circles (triangles) represent flares with complete (incomplete) coverage. Colors represent the SXR burst duration in three bins. The dotted line indicates the best-fit line in linear space that passes through the origin, with a ratio of 0.066, and the dashed lines have slopes that differ by a factor of 2 from the best-fit line.

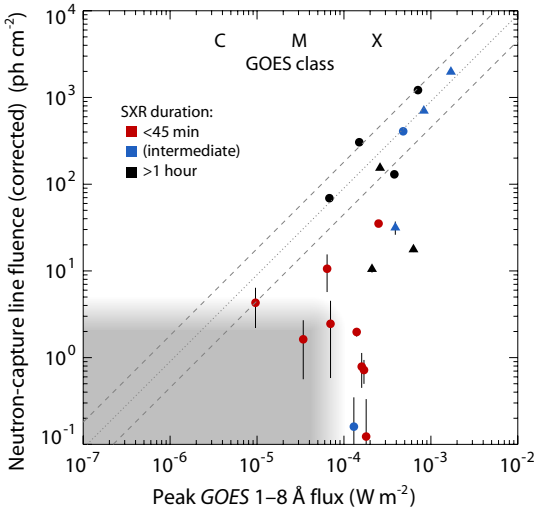

Figure 3. $F_{2.2}$ vs. f_{GOES} for *RHESSI* flares with heliocentric angles $<80°$. The circles (triangles) represent flares with complete (incomplete) coverage. Colors represent the SXR burst duration in three bins. The dotted line and dashed lines (separated by a factor of 2 in slope) illustrate an apparent direct proportionality of the flares with the largest fluences. The shaded area roughly indicates the remaining region of parameter space that has not yet been systematically searched.

a fixed proton power-law spectral index of 3.75 and γ-ray flare composition (see Murphy et al. 2007), and can overestimate the number by up to a factor of $\sim$2 if the true spectral index is different (R. J. Murphy 2009, private communication). We follow Ramaty et al. (1993) to estimate N_e(0.5 MeV), the number of electrons at 0.5 MeV, using each flare's bremsstrahlung spectrum. We obtain particle fluxes J_p(10 MeV) and J_e(0.5 MeV) in particles cm^{-2} s^{-1} MeV^{-1} by multiplying by particle speed, and find that the J_e(0.5 MeV)/J_p(10 MeV) ratios (for the nine complete flares with $>3\sigma$ line fluences) range from $\sim$630 to $\sim$2600 (Table 1) with one (the least significant) at 230. Ramaty et al. (1993) previously found flare ratios of $\sim$1000–10,000.

Figure 3 plots $F_{2.2}$ versus the peak *GOES* 1–8 Å SXR flux, f_{GOES}, emitted by the hot, $\sim 10^7$ K flare thermal plasma. Although in general these emissions are not well correlated ($r^2 = 0.33$ for all flares, $r^2 = 0.18$ for flares with complete coverage), the eight flares with the largest 2.223 MeV line fluences ($F_{2.2} \gtrsim 50$ ph cm^{-2}) show direct proportionality to the *GOES* SXR peak flux to within a factor of about 2. Note that the flares above the threshold have SXR burst durations of >45 minutes. Flares below this threshold typically have large excess f_{GOES} relative to $F_{2.2}$. *SMM* flares (not shown) are consistent with this distribution but exhibit more scatter, as with Figure 2. A preliminary analysis of 13 of the flares (those free of data or background complications) shows that the >50 keV HXR bremsstrahlung fluence, $F_{>50\ \mathrm{keV}}$, observed by *RHESSI* exhibits similar behavior to f_{GOES}: above the same threshold, $F_{2.2}$ is roughly proportional to $F_{>50\ \mathrm{keV}}$, while flares below this threshold generally show large excess $F_{>50\ \mathrm{keV}}$.

3. DISCUSSION

Summarizing the *RHESSI* observations, we find the following close (within a factor of 2) proportionalities:

1. $F_{2.2} = 0.066\ F_{>0.3\ \mathrm{MeV}}$—over >3 orders of magnitude,
2. $F_{2.2} = 9.0 \times 10^9$ ph W^{-1} f_{GOES}—for $F_{2.2} > \sim$50 ph cm^{-2},
3. $F_{2.2} = 1.6 \times 10^{-3}\ F_{>50\ \mathrm{keV}}$—for $F_{2.2} > \sim$50 ph cm^{-2}.

From (1) we infer that the acceleration of relativistic electrons (>0.3 MeV) is proportional to the acceleration of >30 MeV protons, strongly implying a common acceleration mechanism. *SMM* observations show a similar direct proportionality between 4–8 MeV nuclear excess fluences (obtained by subtracting the electron bremsstrahlung power-law continuum, extended from lower energies, from the observed 4–8 MeV fluence) and $F_{>0.3\ \mathrm{MeV}}$, also extending over 3 orders of magnitude in fluences, with $\gtrsim$90% of events within a factor of 2 of the best-fit line (Cliver et al. 1994; Vestrand 1988). The nuclear excess is a combination of narrow and broad nuclear de-excitation lines and the unresolved nuclear continuum, which are typically produced by >2 MeV nuc^{-1} ions.

We do not find a distinct class of electron-dominated flares that produce much more high-energy bremsstrahlung relative to nuclear emission, at least when integrated over the flare. Rieger et al. (1998) found short time intervals within flares that were dominated by electron-associated emission (up to an order of magnitude greater relative emission than typical intervals). In two (2003 November 3 and 2005 September 10) of the *RHESSI* flares that have two well separated time intervals of high-energy emission, the emission from the first interval could be electron-dominated. In both cases, however, the line emission from the second interval is greater, and combining the intervals results in a flare-integrated emission that agrees with the observed proportionality.

From (2) and (3) we infer that the acceleration of nonrelativistic (tens of keV) electrons (and the thermal SXR plasma heated by them) is closely proportional to the acceleration of protons when more than $\sim 2 \times 10^{31}$ protons are accelerated above 30 MeV. Below that threshold, there can be a large excess acceleration of nonrelativistic electrons relative to >30 MeV proton acceleration, and the two processes appear to be uncorrelated. *RHESSI* has observed tens of X-class flares (mostly impulsive) with no significant >0.3 MeV bremsstrahlung or 2.223 MeV line emission.

Cliver et al. (1994) also reported that 4–8 MeV nuclear excess fluences were well correlated to $F_{>50\ \mathrm{keV}}$ (their

Figure 4); they concluded that there is no evidence for a separate high-energy acceleration. However, their Figure 4 is very similar to our Figure 3 in that $F_{>50\ \mathrm{keV}}$ is closely proportional to the 4–8 MeV fluence for flares above a threshold 4–8 MeV fluence ($\sim$10 ph cm^{-2}), while flares below that threshold typically have substantial excess >50 keV fluence relative to 4–8 MeV fluence.

We conclude that the acceleration of >30 MeV protons is always closely proportional to the acceleration of relativistic (>0.3 MeV) electrons, while the acceleration of nonrelativistic electrons is only proportional when the proton acceleration exceeds a threshold. We note that all flares that accelerate enough >30 MeV protons to be detected by *RHESSI* are accompanied by $\sim$M-class or X-class SXR emission; smaller, C-class and lower flares that are "scaled down" versions of the large γ-ray line flares, but without excess >50 keV and SXR thermal emission, are lacking. Note that the smallest flare observed with 2.223 MeV line emission (at $\sim 2\sigma$) is a C4.1 flare observed by *COMPTEL* (Young et al. 2001).

RHESSI made the first images of solar flares in a γ-ray line, and found that 2.223 MeV line emission comes from localized, $\lesssim$35 arcsec, source(s) in the flare (Hurford et al. 2003, 2006), and not from an extended region, as might be expected from widespread acceleration by a shock wave (e.g., Vestrand & Forrest 1993). For the large 2003 October 28 flare, two footpoints straddling the wide flare-loop arcade were detected in the γ-ray line and continuum emission, similar to the HXR footpoints. This is strong evidence that this proportional acceleration of >30 MeV protons and relativistic electrons is also related to magnetic reconnection and the formation of new loops (e.g., Sturrock 1980), similar to the acceleration of tens of keV electrons (e.g., Krucker et al. 2003). Surprisingly, however, the γ-ray line footpoints were separated from the footpoints of the 0.2–0.3 MeV bremsstrahlung continuum by $\sim$10–15 Mm in this and the 2002 July 23 flare.

The observations thus are consistent with two (possibly concurrent) acceleration processes: one that accelerates both ions and electrons proportionally to high energies and a second that accelerates electrons above 50 keV but not above 0.3 MeV. The proportional acceleration appears to occur only in larger, M- or X-class flares, and when more than $\sim 2 \times 10^{31}$ protons are accelerated above 30 MeV, the fraction of energy going to low-energy acceleration and thermal plasma reaches a constant minimum.

To our knowledge, none of the current acceleration theories that treat both ion and electron acceleration predict, a priori, such a closely constrained ratio of >0.3 MeV electrons to >30 MeV protons when integrated over a flare, nor do they predict a close correlation of >50 keV electron acceleration when the >30 MeV proton acceleration exceeds a threshold. Relative acceleration of ions and electrons in the stochastic acceleration models of Miller (2000) or Petrosian & Liu (2004) depends strongly on the size of the acceleration region (see also Emslie et al. 2004a) or on the ratio of the electron plasma frequency to the electron gyrofrequency, respectively. Relative acceleration in direct-electric-field acceleration models (e.g., Dauphin et al. 2007; Zharkova & Gordovskyy 2004) depends strongly on the strength of the guide magnetic field. First-order Fermi acceleration by shocks in the flare loop (e.g., Bai et al. 1983) could couple ion and electron acceleration, but it would depend on the amount of pitch-angle scattering and the processes that accelerate electrons before they interact with the shocks.

The relationship of flare acceleration to SEP acceleration, if any, is still unclear. The J_e/J_p ratios for these γ-ray line flares are about 2 orders of magnitude larger than the ratios for gradual SEP events (Kallenrode et al. 1992; Cliver & Ling 2007), consistent with a different acceleration mechanism for gradual SEP events. Much weaker impulsive SEP events—characterized by emission of lower energy, $\sim$0.1–100 keV electrons and $\sim$0.01–1 MeV nuc^{-1} ions with large enhancements of ^{3}He and heavy elements, and high charge states—are detected far more frequently, over a thousand per year over the whole Sun near solar maximum (Lin 1985). These have J_e/J_p ratios comparable to the flare ratios, consistent with the paradigm that these are due to flare acceleration (Ramaty et al. 1993; Ramaty et al. 1997; Mandzhavidze et al. 1999). However, to our knowledge, impulsive SEP events have rarely, if ever, been detected from a γ-ray line flare, and *RHESSI* did not detect any γ-rays from the flares associated with the impulsive events identified by Reames & Ng (2004) in 2002–2004. Furthermore, many impulsive SEP events have no associated flare, and others appear to be associated with fast ($\sim$1000 km s^{-1}) narrow ($\lesssim 20^\circ$) CMEs (Kahler et al. 2001; Haggerty & Roelof 2002) and/or to jets observed in EUV that occur close to a coronal hole boundary (Wang et al. 2006).

We thank Dr. Gerald Share and Dr. Ronald Murphy for their helpful comments on the manuscript. The research at the University of California, Berkeley, was supported in part by NASA contract NAS5–98033. A. Y. Shih was supported in part by a NASA GSRP Fellowship.

REFERENCES

Bai, T., Hudson, H. S., Pelling, R. M., Lin, R. P., Schwartz, R. A., & von Rosenvinge, T. T. 1983, ApJ, 267, 433
Cane, H. V., McGuire, R. E., & von Rosenvinge, T. T. 1986, ApJ, 301, 448
Cliver, E. W., Crosby, N. B., & Dennis, B. R. 1994, ApJ, 426, 767
Cliver, E. W., & Ling, A. G. 2007, ApJ, 658, 1349
Dauphin, C., Vilmer, N., & Anastasiadis, A. 2007, A&A, 468, 273
Emslie, A. G., Dennis, B. R., Holman, G. D., & Hudson, H. S. 2005, J. Geophys. Res., 110, A11103
Emslie, A. G., Miller, J. A., & Brown, J. C. 2004a, ApJ, 602, L69
Emslie, A. G., et al. 2004b, J. Geophys. Res., 109, A10104
Haggerty, D. K., & Roelof, E. C. 2002, ApJ, 579, 841
Hua, X.-M., & Lingenfelter, R. E. 1987, Sol. Phys., 107, 351
Hurford, G. J., Krucker, S., Lin, R. P., Schwartz, R. A., Share, G. H., & Smith, D. M. 2006, ApJ, 644, L93
Hurford, G. J., Schwartz, R. A., Krucker, S., Lin, R. P., Smith, D. M., & Vilmer, N. 2003, ApJ, 595, L77
Kahler, S. 1994, ApJ, 428, 837
Kahler, S. W., Reames, D. V., & Sheeley, N. R., Jr. 2001, ApJ, 562, 558
Kallenrode, M.-B., Cliver, E. W., & Wibberenz, G. 1992, ApJ, 391, 370
Kiener, J., Gros, M., Tatischeff, V., & Weidenspointner, G. 2006, A&A, 445, 725
Krucker, S., Hurford, G. J., & Lin, R. P. 2003, ApJ, 595, L103
Lin, R. P. 1985, Sol. Phys., 100, 537
Lin, R. P., & Hudson, H. S. 1976, Sol. Phys., 50, 153
Lin, R. P., et al. 2002, Sol. Phys., 210, 3
Lin, R. P., et al. 2003, ApJ, 595, L69
Mandzhavidze, N., Ramaty, R., & Kozlovsky, B. 1999, ApJ, 518, 918
Miller, J. A. 2000, in ASP Conf. Proc. 206, High Energy Solar Physics Workshop—Anticipating HESSI, ed. R. Ramaty & N. Mandzhavidze (San Francisco, CA: ASP), 145
Murphy, R. J., Dermer, C. D., & Ramaty, R. 1987, ApJS, 63, 721
Murphy, R. J., Kozlovsky, B., Share, G. H., Hua, X.-M., & Lingenfelter, R. E. 2007, ApJS, 168, 167
Murphy, R. J., Share, G. H., Letaw, J. R., & Forrest, D. J. 1990, ApJ, 358, 298
Murphy, R. J., Share, G. H., Skibo, J. G., & Kozlovsky, B. 2005, ApJS, 161, 495

Murphy, R. J., et al. 1993, in AIP Conf. Proc. 280, Compton Gamma-Ray Observatory, ed. M. Friedlander, N. Gehrels, & D. J. Macomb (Woodbury, NY: AIP), 619
Petrosian, V., & Liu, S. 2004, ApJ, 610, 550
Ramaty, R., Mandzhavidze, N., Barat, C., & Trottet, G. 1997, ApJ, 479, 458
Ramaty, R., Mandzhavidze, N., & Kozlovsky, B. 1996, in AIP Conf. Proc. 374, High Energy Solar Physics, ed. R. Ramaty, N. Mandzhavidze, & X.-M. Hua (Woodbury, NY: AIP), 172
Ramaty, R., Mandzhavidze, N., Kozlovsky, B., & Skibo, J. G. 1993, Adv. Space Res., 13, 275
Reames, D. V., & Ng, C. K. 2004, ApJ, 610, 510
Rieger, E., Gan, W. Q., & Marschhäuser, H. 1998, Sol. Phys., 183, 123
Schwartz, R. A., Csillaghy, A., Tolbert, A. K., Hurford, G. J., McTiernan, J., & Zarro, D. 2002, Sol. Phys., 210, 165
Smith, D. M., Share, G. H., Murphy, R. J., Schwartz, R. A., Shih, A. Y., & Lin, R. P. 2003, ApJ, 595, L81
Sturrock, P. A. 1980, in Skylab Solar Workshop II, ed. P. A. Sturrock (Boulder: Colorado Associated Univ. Press), 411
Tylka, A. J., & Lee, M. A. 2006, ApJ, 646, 1319
Vestrand, W. T. 1988, Sol. Phys., 118, 95
Vestrand, W. T., & Forrest, D. J. 1993, ApJ, 409, L69
Vestrand, W. T., Forrest, D. J., Chupp, E. L., Rieger, E., & Share, G. H. 1987, ApJ, 322, 1010
Vestrand, W. T., Share, G. H., Murphy, R. J., Forrest, D. J., Rieger, E., Chupp, E. L., & Kanbach, G. 1999, ApJS, 120, 409
Wang, Y.-M., Pick, M., & Mason, G. M. 2006, ApJ, 639, 495
Young, C. A., et al. 2001, in AIP Conf. Proc. 587, GAMMA 2001: Gamma-Ray Astrophysics 2001, ed. S. Ritz, N. Gehrels, & C. R. Shrader (Melville, NY: AIP), 613
Zharkova, V. V., & Gordovskyy, M. 2004, ApJ, 604, 884